Highly stereoselective epoxidation of (−)-α-pinene over chiral transition metal (salen) complexes occluded in zeolitic hosts

Carmen Schuster, Eugen Möllmann, Andras Tompos and Wolfgang F. Hölderich *

Department of Chemical Technology and Heterogeneous Catalysis, University of Technology RWTH Aachen, Worringerweg 1, 52074 Aachen, Germany
E-mail: hoelderich@rwth-aachen.de

Received 13 June 2000; accepted 3 April 2001

Various transition metal complexes of seven different salen ligands have been incorporated in specially modified zeolitic host materials. The thus immobilized sterically demanding complexes have been tested in the diastereoselective epoxidation of (−)-α-pinene in the liquid phase in an autoclave at room temperature and elevated pressure using O_2 as oxidant. In most cases conversions of 100% could be achieved. Best results so far – 100% conversion, 96% epoxide chemoselectivity and 91% diastereomeric excess – have been obtained in the presence of the entrapped [(R,R)-(*N*,*N*′)-bis(3,5-di-*tert*-butylsalicylidene)-1,2-diphenylethylenediamino]cobalt(II) = Co(salen-**5**) complex. Computer simulations were done in order to prove that the reaction can take place inside the pore system, *i.e.*, (−)-α-pinene is able to diffuse through the microporous entrances of the carrier material.

KEY WORDS: heterogeneous catalysis; immobilization; chirality; zeolites; epoxidation; (−)-α-pinene

1. Introduction

Due to the steadily increasing demand for optically pure compounds in the pharmaceutical and agrochemical field the use of chiral catalysts has become a powerful tool in synthetic organic chemistry [1]. Numerous attempts have been made at the immobilization of homogeneous chiral catalysts [2–6]. In this regard, the "ship-in-a-bottle" approach dating back to 1977 offers several advantages over other immobilized homogeneous catalytic systems where the metal complex is attached to a solid surface by covalent or ionic bond [7,8]. The "ship-in-a-bottle" catalyst's main feature is the host–guest interaction which is neither covalent nor ionic. The guest is retained in the zeolite matrix by restrictive pore openings and will, in principle, retain all properties of the homogeneous complex. The superiority of these catalysts to homogeneous systems is based on their easy separation from the reaction mixture and, thus, their relability and environmental compatibility [9]. Furthermore, it is likely that the zeolitic host bestows size and shape selectivity to the catalyst as well as a stabilizing effect on the organometallic complex since, due to the site isolation of the single complexes, multimolecular deactivation pathways such as formation of μ-oxo- or peroxo-bridged species will be rendered impossible [10,11]. Very recently various reports claiming the occlusion of chiral catalysts in the pore structure of faujasite-type zeolites Y and EMT have been published [11–15]. However, even a large-pore zeolite such as zeolite Y, structure of which consists of almost spherical 12 Å supercages interconnected tetrahedrally through smaller apertures of 7.4 Å in diameter [16], is limited regarding the size of guest molecules by the space available in these cavities. Our approach was to enlarge the intrazeolitic cavities in order to generate superior hosts for bulky homogeneous chiral catalysts [11,15]. Such created mesopores which are completely surrounded by micropores offer additional advantages: the entrapped metal complex can move freely and is more accessible during catalysis and even sterically demanding transition states can be formed within the individual pores. The dealumination procedure to generate these materials and the occlusion of Jacobsen's catalyst [(R,R)-(*N*,*N*′)-bis(3,5-di-*tert*-butylsalicylidene)-1,2-cyclohexanediaminato(2-)]manganese(III) chloride = Mn(salen-**2**) (see figure 1) in those hosts have been described previously [11,15].

Now, we succeeded in entrapping the even more bulky [(R,R)-(*N*,*N*′)-bis(3,5-di-*tert*-butylsalicylidene)-1,2-diphe-

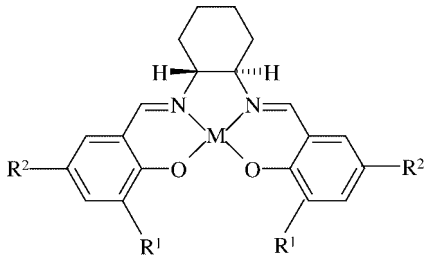

salen-**1**: R^1 = H, R^2 = H
salen-**2**: R^1 = t-Bu, R^2 = t-Bu
salen-**3**: R^1 = t-Bu, R^2 = Me
salen-**4**: R^1 = t-Bu, R^2 = H

Figure 1. Salen complexes derived from (R,R)-cyclohexanediamine.

* To whom correspondence should be addressed.

1011-372X/01/0600-0069$19.50/0

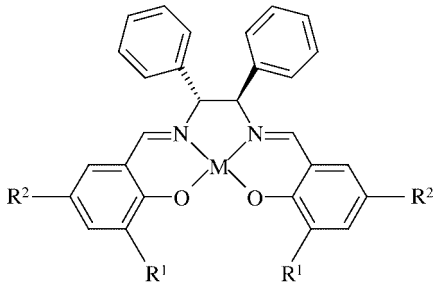

salen-**5**: R^1 = t-Bu, R^2 = t-Bu
salen-**6**: R^1 = t-Bu, R^2 = Me
salen-**7**: R^1 = t-Bu, R^2 = H

Figure 2. Salen complexes derived from (R,R)-diphenylethylenediamine.

nylethylenediamino)transition metal complexes = transition metal-(salen-**5**) complexes (see figure 2). These catalysts have shown very promising results in the stereoselective epoxidation of (−)-α-pinene.

2. Experimental

Zeolites featuring mesopores which are completely surrounded by micropores have been prepared by a combination of two dealumination methods ((1) $SiCl_4$ treatment and (2) steaming). The procedure thereof is described elsewhere [11,15]. Such zeolitic materials were ion-exchanged for 24 h with an aqueous solution of the desired transition metal cation at 353 K. The ion-exchanged material was then dried under vacuum at 523 K (heating rate 1 K/min) and cooled under inert atmosphere prior to ligand synthesis. The ligand synthesis was conducted under inert atmosphere and started with the addition of the optically active diamine in CH_2Cl_2 in excess to the metal loading. After stirring for several hours the appropriate amount of the corresponding aldehyde was added to the slurry and stirring was continued. The solvent was removed and the sample was kept for 12 h at 413 K under vacuum. After cooling to room temperature the remaining solid was soxhlet-extracted for 24 h with CH_2Cl_2 and toluene, respectively, in order to remove surface adsorbed complexes.

2.1. Characterization

The wet chemical analysis was done on an inductive coupled plasma atomic emmision spectroscopy (ICP-AES) Spectroflame D (Spectro). Typically, 30 mg sample was dissolved in 500 μl 40% HF solution, 4 ml 1 : 4 H_2SO_4 solution and 45 ml H_2O.

Infrared Fourier transform spectroscopy (FT-IR) was performed at room temperature on a Nicolet Spectrometer 460 Protégé using standard KBr techniques for the ligands and the homogeneous complexes. The "ship-in-a-bottle" catalysts were prepared as self-supporting wafers.

For thermogravimetric analysis a Netzsch 209/2/E equipped with a STA 409 Controller was used. The heating rate was 1 K/min, using Al_2O_3 crucibles; α-Al_2O_3 was used as reference material.

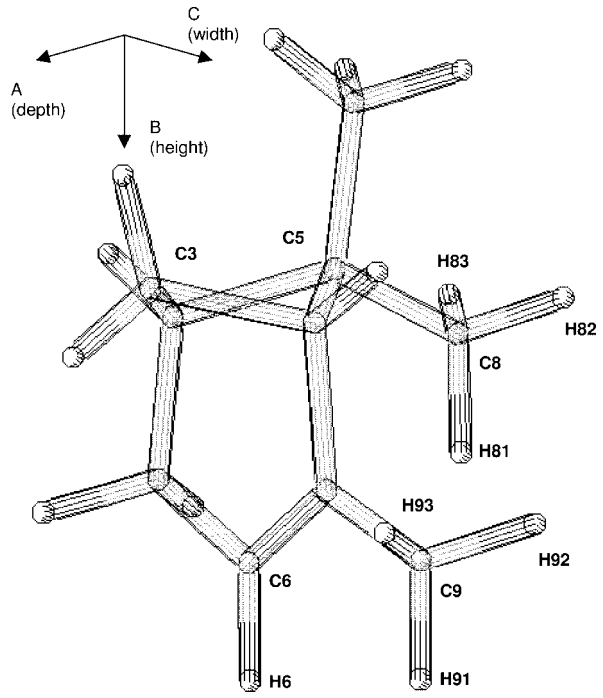

Figure 3. (−)-α-pinene molecule with new coordinate system.

GC analysis was performed on a HP 6890 series gas chromatograph (Hewlett–Packard) using a 60 m 1701 (CPSil 19) column and a 50 m FS-Cyclodex beta-I/P.

2.2. Molecular simulations

The molecular dynamics calculations were done using the DISCOVER molecular simulation program ver. 99.1 together with the INSIGHTII software package from MSI Inc. on a SiliconGraphics Indigo2 workstation. As forcefield PCFF was used. This forcefield is a further development of the second-generation forcefield CFF91 and was parameterized and tested especially on zeolites [17]. The dynamics trajectory of the pinene molecule was calculated at 298 K with a temperature window of 0.5 K using the NVT (= constant particle number, volume and temperature) ensemble. The dynamics of the zeolite was recorded using periodic boundary conditions. In course of the dynamics 20000 conformations were recorded and used to analyze the different geometries.

To determine the size of the pinene molecule a new invariant Cartesian coordinate system was defined, based on three atom positions of the pinene molecule (H6, C6 and C3 in figure 3) after minimization. The size of the pinene molecule was determined by calculating the three largest dimensions perpendicular to each of the three planes of the new coordinate system giving the dimensions of a box enclosing the pinene molecule for every saved conformation.

Starting point for the dynamics calculation of the Y-zeolite was the supplied faujasite structure [18]. As a simplification an all-silicon structure was built by substituting

Al by Si, and afterwards this structure was minimized. The diameter of the microporous pore opening of the Y-zeolite is given by the distance of two adjacent framework oxygen atoms. The van der Waals radius of hydrogen was assumed to be 1.1 Å and of oxygen 1.35 Å. They were provided by the simulation software and are in good agreement with published data [19]. The distributions of the distances d were calculated by counting the distances lying inside an interval of $(d + 0.02)$ Å (n_i) and dividing by the total amount of structures recorded ($N = 20000$). This data was fitted with a non-linear least-squares algorithm to the Gauss function,

$$G(x) = C\sqrt{\frac{\alpha}{\pi}}\exp(-\alpha(x-a)^2), \qquad (1)$$

where C, α and a are the parameters of the fit.

2.3. Catalytical testing

25 mg catalyst, 10 ml fluorobenzene, 0.3 ml (−)-(α)-pinene (1.9 mmol) and 0.5 ml pivalaldehyde (4.6 mmol) in a 75 ml stainless-steel autoclave, 30 bar O_2, 3 h, 25 °C.

3. Results and discussion

Various transition metal complexes of the different salen ligands shown in figures 1 and 2 have been entrapped in the zeolitic host materials. In table 1 the thus prepared catalysts and their properties are summarized.

The "ship-in-a-bottle" catalysts have been characterized by FTIR, ICP-AES, TG-DSC and nitrogen adsorption (BET). Although each ion-exchange was conducted with a 0.01 M solution of the desired metal salt, the metal content of the different heterogeneous catalysts varies. This could be due to the different exchange behavior of the various cations as well as to the amount and location of the remaining framework aluminium in the different batches of highly dealuminated zeolites [20,21]. Ligand loading varies from 1.2 to 12.2 wt%, regardless of the metal loading or the ligand. Ligand loadings were determined using thermogravimetry. Due to their slow decomposition over a broad range of temperature, starting at 523 K and ending at about 823 K, it is not possible to acquire an exact temperature of decomposition for the "ship-in-a-bottle" catalysts. According to our thermogravimetric investigations the free salen ligands as well as the homogeneous Jacobsen catalyst decompose in two steps, the decomposition temperatures being, *e.g.*, 586 and 674 K for the ligand (R,R′)-(*N*,*N*′)-bis(3,5-di-*tert*-butylsalicylidene)-1,2-cyclohexanediamine, and 605 and 694 K for [(R,R′)-(*N*,*N*′)-bis(3,5-di-*tert*-butylsalicylidene)-1,2-cyclohexanediaminato (2-)]manganese(III) chloride. The enhanced thermal stability of the "ship-in-a-bottle" catalysts can be assigned to host–guest interactions of the zeolite and the occluded complex.

Figure 4 shows the FTIR spectra of the (salen-**5**) ligand (A), the homogeneous Co(salen-**5**) complex (B) and the im-

Table 1
"Ship-in-a-bottle" catalyst characterization.

Catalyst	Metal loading[a] (wt%)	Ligand loading[b] (wt%)	Metal/ ligand[c]	IR adsorption characteristic of the complex (cm^{-1})
V(salen-**1**)	0.97	4.4	1.39	1557
Cr(salen-**1**)	0.61	5.4	0.70	1539
Mn(salen-**1**)	0.35	2.8	0.73	1543
Fe(salen-**1**)	0.11	2.7	0.23	1552
Co(salen-**1**)	0.08	2.4	0.18	1557
Rh(salen-**1**)	1.29	4.8	0.84	1553
Ir(salen-**1**)	–	1.2	–	1554
V(salen-**2**)	0.96	3.7	2.78	1550
Cr(salen-**2**)	0.61	5.8	1.10	1537
Mn(salen-**2**)	0.49	6.4	0.76	1533
Fe(salen-**2**)	0.11	5.0	0.21	1556
Co(salen-**2**)	0.14	5.8	0.22	1536
Rh(salen-**2**)	1.28	8.5	0.80	1543
Ir(salen-**2**)	–	2.5	–	1556
Mn(salen-**3**)	0.55	5.3	0.87	1540
Mn(salen-**4**)	0.52	3.9	1.05	1540
Cr(salen-**5**)	1.10	6.0	2.27	1535
Mn(salen-**5**)	0.79	2.4	3.85	1559
Fe(salen-**5**)	1.37	5.7	2.77	1541
Co(salen-**5**)	0.29	8.0	0.40	1540
Rh(salen-**5**)	0.43	12.2	0.22	1541
Ir(salen-**5**)	–	2.2	–	1558
Mn(salen-**6**)	0.38	1.7	2.27	1545
Mn(salen-**7**)	0.36	2.2	1.58	1546

[a] Determination by ICP-AES.
[b] Determination by TG-DSC.
[c] Molar ratio.

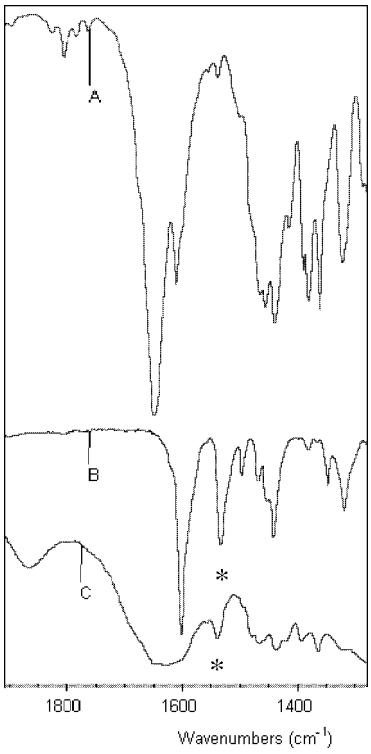

Figure 4. FTIR spectra of (A) the (salen-**5**) ligand, (B) the homogeneous Co(salen-**5**) complex and (C) the immobilized Co(salen-**5**) complex.

Table 2
Nitrogen adsorption investigations.

Sample	BET surface area (m^2/g)	*t*-plot micro-porous volume (cm^3/g)	BJH-meso-porous volume (cm^3/g)
Host (CHZ129)	522.2	0.211	0.113
Mn(salen-**1**)SIB	393.0	0.153	0.102
Mn(salen-**2**)SIB	396.2	0.158	0.098
Mn(salen-**5**)SIB	373.7	0.166	0.064

mobilized Co(salen-**5**) complex (C). The 1540 cm^{-1} absorption characteristic of the homogeneous complex, which can also be found in the spectrum of sample C, indicates the presence of the Co(salen-**5**) complex within the host material.

In order to investigate the transition metal salen complexes' location within the host material we conducted nitrogen adsorption experiments with the empty zeolitic host and with three different immobilized Mn salen complexes. The results are summarized in table 2. In comparison to the host material there can be detected a decrease in the BET surface area and the micro- and mesoporous volumes with all three "ship-in-a-bottle" catalysts. For the Mn(salen-**1**)SIB catalyst, which hosts the smallest among the three entrapped organometallic compounds, the decrease of microporous space is the most prominent, indicating that this complex is mainly located in the zeolite's micropores. In contrast to this, the Mn(salen-**5**) complex, the most bulky of the guest molecules, seems to occupy mainly the mesoporous space of its host. According to the nitrogen adsorption data of the Mn(salen-**2**)SIB catalyst, the guest occupies both micropores and mesopores of the host material, suggesting that major parts of the ligands, *e.g.*, the *tert*-butyl-substituted aromatic groups, stick through the intrazeolitic openings into the microporous space.

Due to the importance of oxygenated monoterpenes as flavor and perfume compounds we investigated the performance of our new chiral catalysts in the oxidation of (−)-(α)-pinene according to

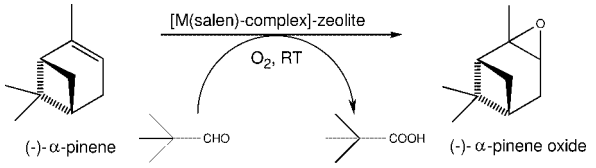

(2)

The benefits of fluorous solvents when using molecular oxygen and pival aldehyde in epoxidation reactions have been described previously [22,23].

A straightforward method of finding out if (−)-(α)-pinene fits through the microporous entrances of the carrier material, is to perform molecular dynamics calculations. From these it is possible to calculate the distribution of dimensions at a given temperature, which are plotted together with the fitted Gauss curves in figure 5.

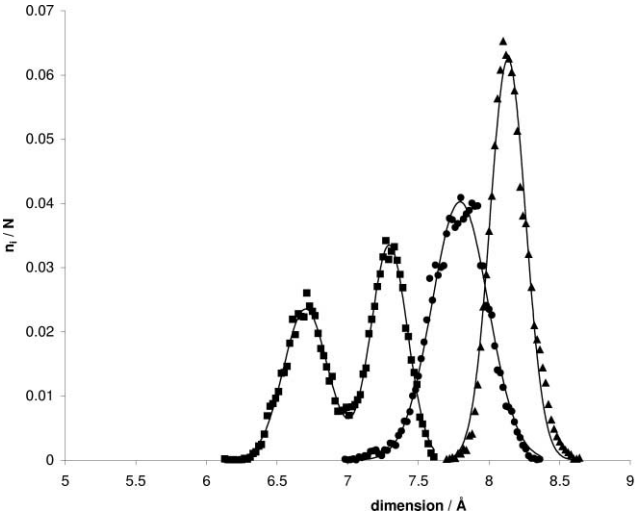

Figure 5. Distribution of the height, width and depth of (−)-α-pinene in course of the molecular dynamics simulation at 298 K. Together with the experimental data, the fitted Gauss curves are represented. (•) Width, (▲) height and (■) depth.

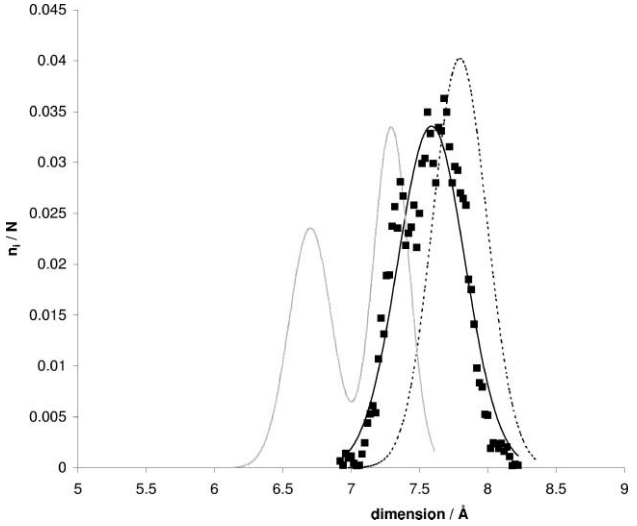

Figure 6. Comparison of the fitted dimensions of (−)-α-pinene with the experimental and fitted data of the pore size. (- - -) Width, ( ) depth and (■) pore size.

The double maximum distribution of the depth can be explained in terms of an at room temperature hindered rotation of the methyl group C8–H81–H82–H83 around the C8–C5 axis allowing two discrete sizes. The same explanation applies for the distorted distribution of the height, where the measured distribution is an unresolved convolution of several normal distributions. On the other hand, the distribution of the width is nicely represented by the fitted curve, which means, that the rotation of the C9–H91–H92–H93 group is unhindered at room temperature.

When comparing the size of molecules with the size of pores, the largest dimension of the molecule is neglected because the molecule will enter the pores through their smallest dimensions [24]. In the case of (−)-(α)-pinene the largest dimension is the height, with a fitted most probable diameter

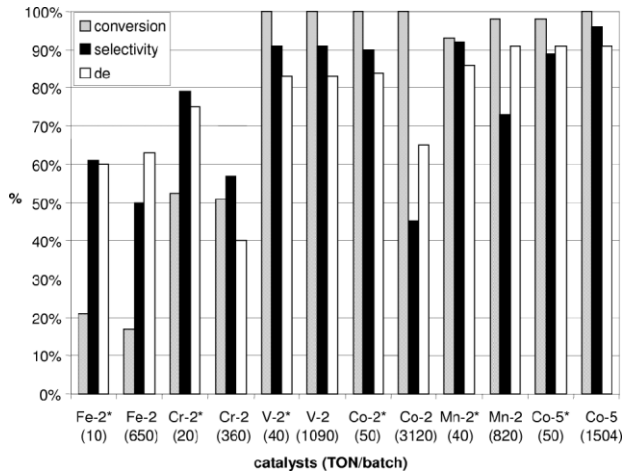

Figure 7. Epoxidation of (−)-α-pinene in the presence of various homogeneous and immobilized transition metal(salen) complexes. ∗ = homogeneous complex.

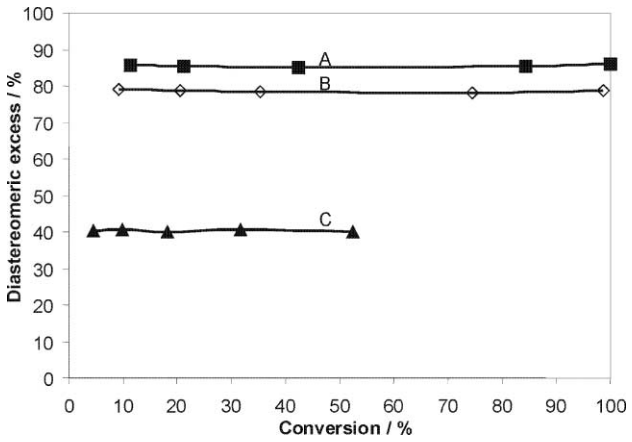

Figure 8. Diastereomeric excess–conversion dependencies in the epoxidation reaction of (−)-α-pinene in the presence of immobilized transition metal (salen) complexes. Reaction with (A) Co-**1**, (B) Mn-**3** and (C) Cr-**2** complexes.

of 8.13 Å. In figure 6 the width and depth of (−)-(α)-pinene are compared with the pore size.

The fitted pore size distribution shows a most probable value of 7.59 Å with a standard deviation of 0.25 Å. From that one can calculate, that 95.5% of the time, the pore size should lie in the range (7.59 ± 0.5) Å. It can be clearly seen, that the depth distribution of (−)-(α)-pinene falls in this range or is even smaller. Also the width of (−)-(α)-pinene lies with a probability of more than 90% in the appropriate pore size range, so that it is proven, that the microporous openings of the faujasite are no significant hindrance for the diffusing (−)-(α)-pinene molecule towards the homogeneous metal salen complex entrapped in the mesopores.

The catalytic results summarized in figure 7 show that in the oxidation of (−)-(α)-pinene the homogeneous and heterogeneous (salen-**2**) complexes of V, Co and Mn and Co(salen-**5**) complexes achieved high conversion and, apart from the heterogeneous Co(salen-**2**) complex, high selectivity and high diastereomeric excess (de). The best results were obtained with the heterogeneous Co(salen-**5**) complex, its performance with 96% selectivity and 91% de at 100% conversion was even better than that of its homogeneous counterpart. Second best of the "ship-in-a-bottle" catalysts was the V(salen-**2**) complex with regard to selectivity and the Mn(salen-**2**), the heterogenized Jacobsen catalyst, with regard to diastereoselectivity. An explanation as to why the catalytic performance of the entrapped Co(salen-**2**) complex is less efficient than its homogeneous counterpart cannot be given so far. The complexes of Fe and Cr achieved low to moderate conversion, moderate selectivity and diastereomeric excess. In contrast to results published earlier, the majority of the guest complexes have been entrapped without considerable loss of their catalytic performance [11,15]. In the heterogeneous systems – presumably because of the site isolation of the immobilized organometallic complexes – no deactivation of the catalysts takes place, which leads to apparently higher turnover numbers as given in figure 7. It should be also emphasized that the catalysts were reused four times without loss of activity, which results in the total turnover number being at least four times higher than the numbers given in the figures. In order to investigate if our zeolite contributes to the product spectrum other than to serve as host we conducted several catalytic experiments with the unloaded zeolite as well as with the metal-exchanged material prior to ligand synthesis. According to GC analysis no reaction took place and to our best knowledge there is no literature information concerning the epoxidation of (−)-(α)-pinene to (−)-(α)-pinene oxide in the presence of metal-exchanged zeolitic materials. Nevertheless, the possibility of an interaction of remaining acid sites with the entrapped transition metal complexes cannot be excluded completely.

To check the influence of the product on the diastereomeric excess, the reaction mixture was analysed at different conversion levels. Figure 8 contains the diastereomeric excess–conversion dependencies obtained in the presence of three different "ship-in-a-bottle" catalysts. As emerges from the data none of the products seems to have an effect on the further reactions.

Due to the excellent catalytic results obtained in the epoxidation of (−)-α-pinene with the immobilized Co(salen-**5**) complex (figure 9) we entrapped a variety of transition metal complexes of the salen-**5** ligand and investigated their catalytic behavior under the same reaction conditions. The results, as depicted in figure 9, indicate that except for the Co(salen-**5**) complex only the corresponding manganese complex exhibits promising potential. For example the (salen-**5**) complexes of Cr and Fe gave only modest conversion and all catalysts, with exception of the Co and Mn species, achieved at the very best moderate product and stereoselectivities.

The catalytic behavior of various entrapped transition metal(salen-**1**) complexes are shown in figure 10. Best results are achieved with the manganese complex, *i.e.*, 100% conversion, 83% selectivity and 79% de. Conversion and diastereoselectivity are lowest when employing the corresponding Rh and Ir complexes, but with regard to chemo-

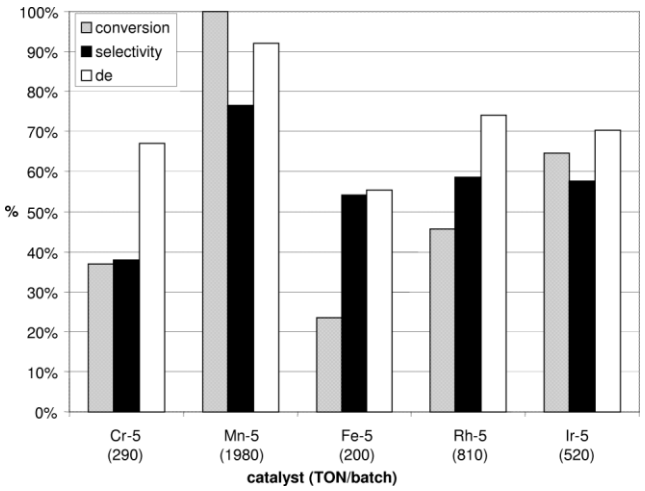

Figure 9. Epoxidation of (−)-α-pinene in the presence of various immobilized transition metal (salen-**5**) complexes.

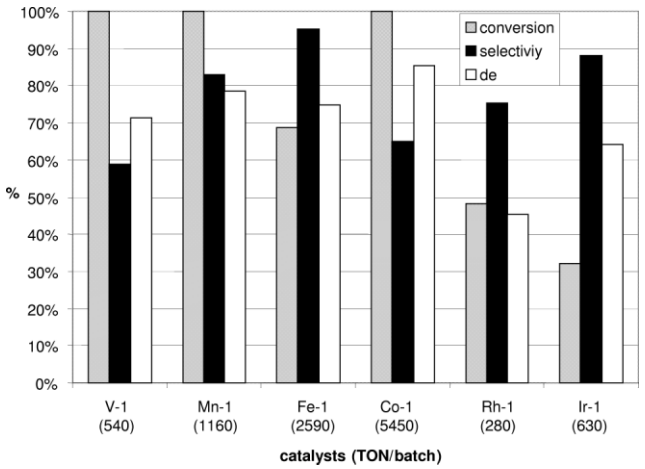

Figure 10. Epoxidation of (−)-α-pinene in the presence of various immobilized transition metal (salen-**1**) complexes.

selectivity the Ir(salen-**1**) catalyst obtained the second best results (88%) of the occluded salen-**1** catalysts.

We studied the catalytic behavior of seven different entrapped Mn(salen) complexes (figures 1 and 2) in the epoxidation of (−)-α-pinene, too. The results, as summarized in figure 11, show that all catalysts achieved high conversion (>95%). Surprisingly, with regard to chemo- and stereoselectivity, the best results of this study were obtained with the immobilized manganese complexes of salen-**4** and salen-**5** and not, as one might expect, with the occluded Jacobsen catalyst Mn(salen-**2**). Taking into consideration the observations made in the discussion of figure 4, *i.e.*, neither the homogeneous nor the immobilized Jacobsen complex achieved the best catalytic results among their respective (salen-**2**) counterparts, it can be assumed that Jacobsen's catalyst is not particularly suited for the epoxidation of (−)-α-pinene.

To establish the lack of leaching of the complex, we performed chemical analysis of the liquid after reaction. No metal ions could be detected. We further investigated the

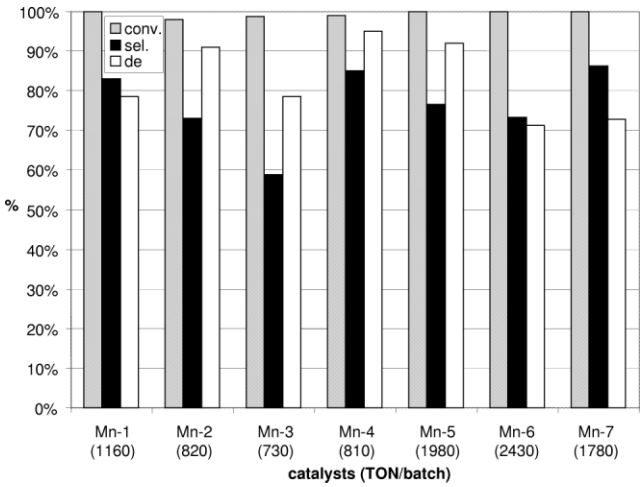

Figure 11. Epoxidation of (−)-α-pinene in the presence of various immobilized Mn(salen) complexes.

aspect of leaching as suggested by Sheldon *et al.* [25] by separating the catalyst from the reaction mixture by filtration prior to total olefin consumption. The filtrate was stirred additionally for several hours under reaction conditions. According to GC analysis no further reaction had occurred after filtration of the "ship-in-a-bottle" catalyst, indicating that our new heterogeneous catalysts do not leach.

4. Conclusion

A number of transition metal complexes of seven different salen ligands have been occluded in a zeolitic host material featuring mesopores which are completely surrounded by micropores. These "ship-in-a-bottle" catalysts have been characterized by means of FT-IR spectroscopy, ICP-AES and TG-DSC. The catalytic behavior of the entrapped bulky transition metal complexes has been investigated in the stereoselective epoxidation of (−)-α-pinene. Molecular simulations showed, that (−)-(α)-pinene is a suited substrate for this reaction, because the surrounding micropores of the carrier material do not block the (−)-(α)-pinene from the active sites. A comparison of the respective catalytical results of the new heterogeneous catalysts and their homogeneous counterparts showed that the entrappment of the organometallic complex was achieved without considerable loss of activity and selectivity. In contrast to their homogeneous counterparts, the immobilized catalysts are reusable. Their catalytically active compound does not leach. Furthermore, the use of molecular oxygen instead of NaOCl as the oxidizing agent makes our catalytic system more environmentally benign than the system applied by Jacobsen and coworkers. Furthermore, a deactivation of the homogeneous Jacobsen catalyst, due to, for example, decomposition or dimerisation, was not observed after occluding it in the zeolitic framework and working in the presence of oxygen. The best results so far – 100% conversion, 96% selectivity and 91% diastereomeric excess – were achieved with the immobilized cobalt(salen-**5**) complex.

Acknowledgement

The authors are very grateful to the Deutsche Forschungsgemeinschaft (DFG), Sonderforschungsbereich 380, for financial support of this work.

References

[1] R.A. Sheldon, *Chirotechnology* (Dekker, New York, 1993).
[2] J.A. Mayoral, J.M. Fraile, J.I. Carcía and J. Massam, J. Mol. Catal. A 136 (1998) 47.
[3] M. Corma, F. Iglesias, F. Mohino and J. Sánchez, Organomet. Chem. 544 (1997) 147.
[4] G.J. Kim and S.H. Kim, Catal. Lett. 57 (1999) 139.
[5] P. Piaggio, P. McMorn, C. Langham, D. Bethell, P.C. Bulman-Page, F.E. Hancock and G.J. Hutchings, New J. Chem. (1998) 1167.
[6] I.F.J. Vankelecom, D. Tas, R.F. Parton, V. Van de Vyver and P.A. Jacobs, Angew. Chem. 108 (1996) 1445; Angew. Chem. Int. Ed. Engl. 35 (1996) 1346.
[7] B.V. Romanovskii and V.Y. Zakharov, Vestn. Mosk. Univ. Khim. 18 (1977) 142.
[8] G. Schulz-Ekloff, G. Meyer, D. Wöhrle and M. Mohl, Zeolites 4 (1984) 30.
[9] P.A. Jacobs, R. Parton and D. de Vos, in: *Zeolite Microporous Solids: Synthesis, Structure, and Reactivity*, ed. E.G. Derouane (Kluwer Academic, Dordrecht, 1992) p. 555.
[10] K.J. Balkus, Jr., A.K. Khanmamedova, K.M. Dixon and F. Bedioui, Appl. Catal. 143 (1996) 159.
[11] C. Heinrichs and W.F. Hölderich, Catal. Lett. 58 (1999) 75.
[12] W. Kahlen, A. Janssen and W.F. Hölderich, in: *Stud. Surf. Sci. Catal.*, Vol. 108, eds. H.U. Blaser, A. Baiker and R. Prins (Elsevier, Amsterdam, 1997) p. 469.
[13] W. Kahlen, H.H.W. Wagner and W.F. Hölderich, Catal. Lett. 54 (1998) 85.
[14] T. Bein and S.B. Ogunwumi, J. Chem. Soc. Chem. Commun. (1997) 901.
[15] C. Schuster and W.F. Hölderich, Catal. Today 60 (2000) 193.
[16] M.S. Rigutto, in: *Stud. Surf. Sci. Catal.*, Vol. 58, eds. H. van Bekkum, E.M. Flanigen and J.C. Jansen (Elsevier, Amsterdam, 1991) p. 729.
[17] J.-R. Hill and J. Sauer, J. Phys. Chem. 98 (1994) 1238.
[18] D.H. Olson, J. Phys. Chem. 74 (1970) 2758.
[19] Ch. Song, X. Ma, A.D. Schmitz and H.H. Schobert, Appl. Catal. A 182 (1999) 175.
[20] C.Y. Li and L.V.C. Rees, Zeolites 6 (1986) 51.
[21] R.P. Townsend, in: *Stud. Surf. Sci. Catal.*, Vol. 58, eds. H. van Bekkum, E.M. Flanigen and J.C. Jansen (Elsevier, Amsterdam, 1991) p. 359.
[22] T. Mukaiyama, T. Yamada, K. Imagawa and T. Nagata, Chem. Lett. (1992) 2231.
[23] J.-P. Bégué, F. Barbier, K.S. Ravikumar and D. Bonner-Delpon, Tetrahedron 54 (1998) 7457.
[24] R.Ch. Deka and R. Vetrivel, J. Catal. 174 (1998) 88.
[25] R.A. Sheldon, I.W.C.E. Arends, M. Wallau and U. Schuchard, Acc. Chem. Res. 31 (1998) 485.